Bioactive Materials 14 (2022) 443–455

Contents lists available at ScienceDirect

Bioactive Materials

journal homepage: www.keaipublishing.com/en/journals/bioactive-materials

Application of antibody-conjugated small intestine submucosa to capture urine-derived stem cells for bladder repair in a rabbit model

Yu-Ting Song [a,1], Yan-Qing Li [a,1], Mao-Xuan Tian [a,b,1], Jun-Gen Hu [a], Xiu-Ru Zhang [a,c], Peng-Cheng Liu [a,d], Xiu-Zhen Zhang [a], Qing-Yi Zhang [a], Li Zhou [e], Long-Mei Zhao [a], Jesse Li-Ling [a,f], Hui-Qi Xie [a,*]

[a] Laboratory of Stem Cell and Tissue Engineering, Orthopedic Research Institute, Med-X Center for Materials, State Key Laboratory of Biotherapy, West China Hospital, Sichuan University, Chengdu, Sichuan, 610041, China
[b] Department of Aesthetic Surgery, The People's Hospital of Pengzhou, Chengdu, Sichuan, 611930, China
[c] Surgery of Spine and Spinal Cord, Henan Provincial People's Hospital, Zhengzhou, Henan, 450000, China
[d] Department of Burn and Plastic Surgery, West China Hospital, Sichuan University, Chengdu, Sichuan, 610041, China
[e] Research Core Facility of West China Hospital, Sichuan University, Chengdu, Sichuan, 610041, China
[f] Department of Medical Genetics and Prenatal Diagnosis, West China Second Hospital, Sichuan University, Chengdu, Sichuan, 610041, China

ARTICLE INFO

Keywords:
Regenerative medicine
Bladder tissue engineering
Scaffold
Antibody-conjugated
Stem cell capture

ABSTRACT

The need for bladder reconstruction and side effects of cystoplasty have spawned the demand for the development of alternative material substitutes. Biomaterials such as submucosa of small intestine (SIS) have been widely used as patches for bladder repair, but the outcomes are not fully satisfactory. To capture stem cells *in situ* has been considered as a promising strategy to speed up the process of re-cellularization and functionalization. In this study, we have developed an anti-CD29 antibody-conjugated SIS scaffold (AC-SIS) which is capable of specifically capturing urine-derived stem cells (USCs) *in situ* for tissue repair and regeneration. The scaffold has exhibited effective capture capacity and sound biocompatibility. *In vivo* experiment proved that the AC-SIS scaffold could promote rapid endothelium healing and smooth muscle regeneration. The endogenous stem cell capturing scaffolds has thereby provided a new revenue for developing effective and safer bladder patches.

1. Introduction

Bladder is an important organ responsible for urine storage and coordination of micturition through contraction. Trauma, tumor resection, congenital defect, and systemic diseases can all result in bladder defects which may necessite bladder reconstruction through surgery. Meanwhile, the selection of grafting tissue has remained as a major challenge for reconstructive urology. Implants for urinary reconstruction should be readily available and viable in the urinary environment. At present, mucosal grafts or skin grafts have been used for the purpose of ureteral reconstruction [1–3], while neobladder or bladder augmentation cystoplasty using a gastrointestinal segment is the most commonly used therapeutic option [4,5]. However, such procedures are often accompanied by various complications including urinary tract infection, bladder calculi, and metabolic disorders, which may compromise the effect of treatment and life quality of the patients [6,7].

Advances in tissue engineering and regenerative medicine have enabled scientists to develop more promising and revolutionary treatment strategies for bladder regeneration [8]. Ongoing strategies for the regeneration of defective and/or lost tissues have based on construction of biological scaffolds by using pliable scaffolds which can mimic the active and passive bi-axial mechanical properties of the organ in combination with stem cells for tissue regeneration [9–12]. Direct seeding stem cells onto the scaffolds to fabricate a patch for bladder repair has become a commonly used strategy [13–16]. However, poor viability and survival rate of the transplanted cells have affected the efficacy of such therapies as well as raised safety concerns [17]. Selective capture of autologous cells with specific antibody-crosslinked microchip, scaffold

Peer review under responsibility of KeAi Communications Co., Ltd.
* Corresponding author. Laboratory of Stem Cell and Tissue Engineering, Orthopedic Research Institute, Med-X Center for Materials, State Key Laboratory of Biotherapy, West China Hospital, Sichuan University, Chengdu, 610041, China.
E-mail address: xiehuiqi@scu.edu.cn (H.-Q. Xie).
[1] Yu-Ting Song, Yan-Qing Li and Mao-Xuan Tian have contributed equally to this article.

https://doi.org/10.1016/j.bioactmat.2021.11.017
Received 29 August 2021; Received in revised form 26 October 2021; Accepted 12 November 2021
Available online 27 November 2021

and/or platform has been tried for disease diagnosis and treatment [18–21], which has proven to be a promising strategy for tissue repair.

USCs are a novel type of MSCs derived from urine samples in recent years [22,23]. Compared with MSCs from other sources, USCs have several advantages: (1) the source of MSCs such as adipose-derived stem cells (ASCs) and bone marrow mesenchymal stem cells (BMSCs) are limited and the acquisition process are invasive, whereas USCs can be collected from urine noninvasively [24,25]; (2) The isolation of MSCs samples from other sources is complicated and requires enzyme digestion process, and the cell expansion also takes a long time. However, USCs can be isolated using a relatively simple method and be easily cultivated [26,27]; (3) USCs have telomerase activity and cytogenetics stability, allowing high cell proliferation without the risk of tumourigenesis [22,26,28]; (4) USCs isolated from autologous urine do not express HLA-DR responsible for triggering the immune response and could not cause the immune response or rejection [24,29]. Previous studies have shown that the USCs may originate from renal tubules or papillae [22,28,30], and can differentiate into smooth muscle lineage (mesodermal origin) and urothelial lineage (endodermal origin) *in vitro* [23,26,31]. Being highly homologous to the urinary system [22,32], the USCs can better adapt to the environment of bladder *in vivo*, and have therefore been considered as an ideal cell source for bladder tissue regeneration and reconstruction. Endogenous USCs in urine may therefore be captured by bladder repair materials and provide an unlimited source of cells for bladder regeneration and repair.

Based on above notions, we have designed a urine derived stem cells (USCs) capturing scaffolds for bladder repair and regeneration. A well established and off-the-shelf scaffold, small intestine submucosa (SIS), was used as the patch biomaterial. Anti-CD29 antibody, once crosslinked with the SIS, can specifically and synergistically promote the capture of CD29 positive stem cells. The engineered surface was expected to capture the USCs and promote their proliferation and differentiation into the epithelium and smooth muscle *in situ*, and hence facilitate bladder repair and regeneration.

2. Materials and methods

2.1. Preparation of antibody-conjugated SIS

For the preparation of antibody-conjugated SIS (AC-SIS), chemical conjugation of the SIS with the antibody was realized by a two-step reaction with sulfo-succinimidyl derivatives (Sulfo-SMCC, Sigma-Aldrich, USA) and Traut's Reagent (2-Iminothiolane• HCl, Sigma-Aldrich, USA).

Briefly, various concentrations of the Traut's Reagent (0, 0.625, 1.25, 2.5, 5, 7.5, 10 mg/mL were dissolved into phosphate-buffered saline (PBS; ZSGB-BIO, China) with 2 mg/mL of EDTA (pH = 8.0). The SIS (2 cm in diameter) was then soaked into the Traut's Reagent for 1.5 h at room temperature. To analyze the effectiveness of the Traut's Reagent on the SIS, Ellman's Reagent (Sigma-Aldrich, USA) was used to quantify the sulfhydryl (SH) groups. After fully reacting with the Traut's Reagent, the SIS was reacted with 300 μL of Ellman's Reagent (4 mg/mL) in 1 mM Na_3PO_4 solution (pH = 8.0) at room temperature for 15 min. The absorbance was measured at 412 nm with a plate reader (Tecan, Sunrise, Australia). The absorbance was transformed into the amount of sulfhydryl (SH) groups based on the calibration curve of acetylcysteine (Sigma-Aldrich, USA) using the Ellman's Reagent. For detecting the binding capacity of CD29 on the SIS, serial concentrations of antibody (5 μg, 10 μg and 20 μg) were diluted with PBS containing 2 mg/mL of EDTA (pH = 8.0) and reacted with Sulfo-SMCC (0.5 mg/mL) at room temperature for 1 h, which was then washed by PBS for three times.

The SIS treated by the Traut's Reagent was washed with PBS for three times, and incubated with antibodies treated by Sulfo-SMCC for 1 h at room temperature (Fig. 1). The SIS was then washed with PBS for several times and incubated with 5% (W/V) Glycin (Ameresco, USA) and 5% (W/V) bovine serum albumin (BSA) (Sigma-Aldrich, USA) for 3 h to block the remaining reaction. The CD29 conjugated SIS was named as AC-SIS.

2.2. Assessment of CD29 antibody crosslinking

After the CD29 antibody crosslinking, the remaining reaction solution was collected to determine the rate of cross-linking. The concentration of residual CD29 antibody was determined with an anti-mouse IgG ELISA kit (Santa Cruz, USA). The cross-linking rate was determined with a calibration curve based on known concentrations of CD29.

Biotin-labeled goat anti-mouse IgG (H + L, Abcam, UK) was used to label the mouse anti-human primary antibody conjugated to the SIS. The signals were amplified with horseradish peroxidase-labeled streptavidin, and a DAB solution was used for color development.

2.3. Morphological analysis

Surface morphologies of the SIS and AC-SIS were examined with a Field Emission Scanning Electron Microscope (EVO 10, Carl Zeiss AG, Germany) operated at 20 kV. Freeze-dried samples were sputter coated with Au and observed at 500 × magnification.

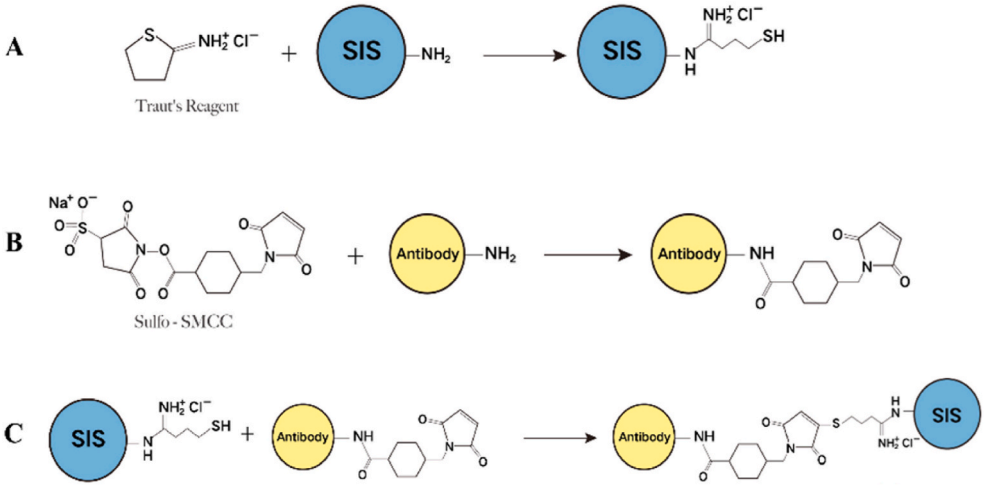

Fig. 1. Schematic representation of chemical crosslinking of antibody with the SIS.

2.4. Measurement of contact angle

Contact angle of the materials was detected with a Kruss goniometer (DSA25, Germany) at 20 °C. Dropped deionized water was added onto the sample surface. Five pictures were recorded and analyzed with the equipped DSAI software.

2.5. Measurement of mechanical properties

The SIS and AC-SIS were cut into rectangle shape (2 cm × 10 cm, n = 5). Elastic modulus of the samples was tested under dry condition with an uni-axial testing machine (Instron 8874, USA). The tests were performed with a stretch rate of 10 mm/min till the samples were cracked. The elastic modulus was calculated by measuring the slope of the stress-strain curve.

2.6. Primary culture of the USCs and flow cytometry analysis

Primary culture of the USCs was performed as previously described [33,34]. Briefly, the USCs were obtained from four young male adult donors (20–30 years old). Fresh urine sample (about 200 mL) was centrifuged and washed with PBS for twice. The sediment was re-suspended and cultured in T25 cell culture flasks with 5 mL of established medium [35].

Cells in logarithmic growth phase were digested with trypsin (Gibco, USA), with their density adjusted to 1×10^6 cells/mL with PBS. 100 μL aliquot of cell suspension was moved to each flow tube (Corning, USA). Thereafter, 2 μL of mouse anti-human CD29 (559883, BD Pharmingen™, USA), mouse anti-human CD34 (555821, BD Pharmingen™), mouse anti-human CD44 (555478, BD Pharmingen™), mouse anti-human CD73 (550257, BD Pharmingen™), mouse anti-human CD90 (561558, BD Pharmingen™) and mouse anti-human CD133(130-111-085, Miltenyi Biotec GmbH, Germany) antibodies were added to each tube. The mixture was allowed to incubate for 30 min in darkness at room temperature. Thereafter, the cells were washed twice with PBS and re-suspended in 200 μL PBS for flow analysis.

2.7. Differentiation induction of the USCs

Adipogenic, osteogenic, and chondrogenic differentiation of the USCs was performed as previously described [33,35].

As for urothelium differentiation, 4×10^3 USCs were seeded onto a 12-well plate (Corning, USA) and cultured in K-SFM medium (Gibco, USA) containing 2% fetal bovine serum (FBS, Gibco, USA) and 30 ng/mL of epidermal growth factor (EGF) (Gibco, USA) for 21 days. For smooth muscle differentiation, 4×10^3 USCs were cultured in 80% DMEM (Gibco, USA) and 15% F12 medium containing 5% FBS, 2.5 ng/mL transforming growth factor beta1 (TGF-β1), 5 ng/mL platelet-derived growth factor subunit BB (PDGF-BB) for 28 days. The induction medium was replaced every 2 days. The induced cells were identified by immunofluorescence (IF) staining for urothelium-specific markers AE1/AE3 (ab9377, Abcam), smooth muscle-specific markers α-SMA (ab32575, Abcam) and Myosin (ab11083, Abcam). Uninduced USCs were used as the control.

2.8. Effect of CD29 antibody on cell proliferation

For evaluating the effect of antibody on the proliferation capacity of USCs, 100 μL of CD29 antibody (10 μg/mL; 556047, BD Pharmingen™) was added to the 96-well plate and coated overnight at 4 °C. Thereafter, 4×10^4 cells were added to each plate. Proliferation of the cells was assessed with a Cell Titer 96 Assay kit (Promega, USA) in 1, 3 and 5 days.

2.9. USCs captured by the AC-SIS in vitro

To evaluate their ability for capturing the USCs, the SIS and AC-SIS scaffolds were compared under static and dynamic circumstances.

Under the static condition, the SIS and AC-SIS were respectively placed in 24-well culture plates containing 1 mL of USCs suspension (2×10^4 cells) per well. After 30 min, cell suspension was removed, and the plates were washed 3 times with PBS. The materials inoculated with the USCs were then transferred to a new plate and cultured in an incubator (Fig. 2). Viability of the captured cells was assessed though proliferation capacity and fluorescence. Proliferation of the captured cells was recorded at days 1, 3 and 5 using a Cell Counting Kit-8 (Dojindo Molecular Technologies, Japan) at 450 nm (OD_{450}) or labeled with 1 μg/mL of calcein-AM (Sigma, USA) for 45 min at 37 °C and observed and photographed under light and fluorescence microscopes (Olympus, Japan).

Under the dynamic condition, an extracorporeal suspension system [30] was used to simulate the USCs transfer process in urine (Supplementary material video). USCs (P3) labeled with CM-Dil (C7000, Invitrogen, USA) were prepared. The suspension cell culture flask was filled with the USCs at 2×10^4 cells/100 mL to simulate the storage and excretion of USCs in urine *in vivo*. The SIS and AC-SIS were respectively hung in the culture flasks containing suspension of CM-Dil-labeled USCs for 24 h. Non-adhered cells were gently washed off with PBS.

With the above method, the SIS and AC-SIS were suspended in the USCs suspension for 6 h and 24 h, and removed for cytoskeleton staining thereafter. The scaffolds were washed with PBS at 37 °C and fixed with 4% paraformaldehyde for 10 min at room temperature. Actin cytoskeleton was stained with FITC-phalloidin (P5282, Sigma-Aldrich, USA). Cell nuclei were stained with DAPI (C1005, Beyotime, China). All samples were observed and photographed under a confocal laser scanning microscope (Nikon, Japan).

2.10. Biocompatibility of the SIS and AC-SIS

Biocompatibility of the scaffolds was quantified. The SIS and AC-SIS (2 cm in diameter) were paved into a 12-well plate. 1 mL of USCs suspension (5×10^4 cells/mL) were seeded in each well, and the medium was replaced every day. After 3 days, the cells were digested and collected. 200 μL of cell suspension was incubated with 2 μL Annexin V/P (Keygen, China) at 4 °C for 5 min. After being washed 3 times with PBS, the samples were detected with flow cytometry (Becton Dickinson, USA).

With the above method, after the USCs were cultured for three days, the scaffolds were harvested and fixed with 2.5% glutaraldehyde for 30 min and dehydrated through an alcohol gradient, coated with Au, and visualized with SEM.

2.11. Animal experiments

All animal experimental procedures were approved by the Sichuan University Animal Care and Use Committee in concordance with the Principles of Laboratory Animal Care formulation by The National Society for Medical Research.

36 male healthy New Zealand white rabbits (purchased from Animal Center of Sichuan Province) which initially weighted 3.0 ± 0.2 kg were used for the experiment. The animals were randomized divided into sham, SIS and AC-SIS groups, with three rabbits used for each time point. The bladders of anesthetized rabbits were exposed through injection of pentobarbital sodium (2 mL/kg) through the marginal auricular vein. As shown in Fig. S1, a paramedian incision was made in the abdomen of each rabbit. A 2 cm × 2 cm full-thickness square defect was then made in the posterior wall of bladder.

An absorbable thread was used to fix the control group with diagonal suture, and whole layer suture was made to form a linear defect. A sterilized SIS or AC-SIS patch (2.2 cm × 2.2 cm in size) was sewn into place with degradable sutures (5-0 Monocryl, Johnson & Johnson, USA). Non-absorbable sutures (5-0 Monocryl) were used to mark the defect area in the sham and experiment groups, and closed the abdomen layer

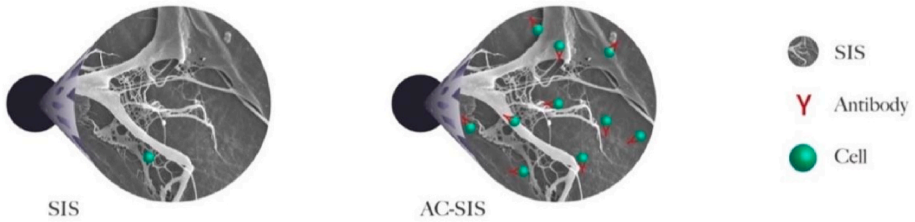

Fig. 2. Schematic representation of AC-SIS specifically capture of USCs.

by layer. The animals were sacrificed by injection of air at 1, 2, 4 and 8 weeks.

2.12. Histological and immunofluorescence analyses

Tissue samples were fixed with 10% neutral formaldehyde, embedded in paraffin, and sectioned in 5 μm diameter specimen, which was followed by HE staining for the observation of material degradation, morphological and histological changes and process of re-epithelialization, and Masson staining for the observation of muscle tissue regeneration.

AE1/AE3 (ab9377, Abcam) antibody was used to observe the re-epithelialization of full-thickness of rabbit bladder. Myosin (ab11083, Abcam) and α-SMA (ab32575, Abcam) were used to observe the regeneration of bladder muscle.

2.13. Statistical analysis

All values are presented as mean ± SD. Statistical analysis was carried out using the student's t-test or one-way ANOVA with Tukey's test *post hoc*. $P < 0.05$ was considered to be statistically significant.

3. Results

3.1. Preparation and basic characteristics of the AC-SIS

To achieve specific identification and capture of scaffold materials, the SIS was conjugated with antibody for the highly expressed marker CD29 based on identification of rUSCs surface markers [34].

The Ellman's Reagent assay was used to determine the sulphydryl grafting efficiency of the Traut's Reagent on the SIS. Along with the increase in Traut's Reagent concentration, the number of sulphydryl groups on the material has also increased until the concentration was above 5 mg/mL (Fig. 3A). Based on the result, 5 mg/mL Traut's Reagent

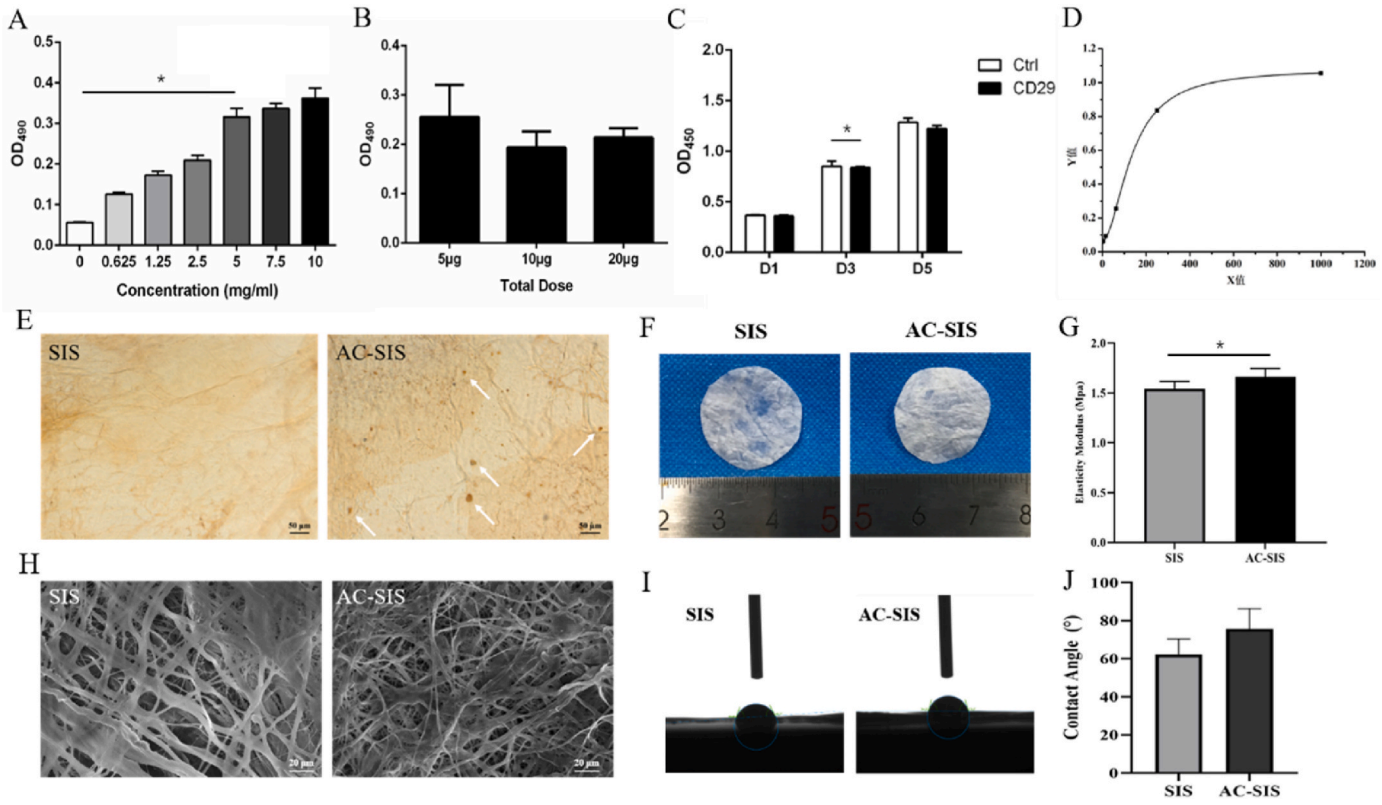

Fig. 3. Determination of the cross-linking condition and analysis of the structure and mechanical properties of the AC-SIS. (A) Measurement of sulfhydryl graft absorbance of the SIS with various concentrations of Traut's Reagent. *$P < 0.05$. (B) Measurement of remaining sulfhydryl absorbance after cross-linking with various concentrations of CD29 antibody. (C) Cell proliferation with 10 μg/mL of CD29 antibody as detected with a Cell Titer 96 kit. (D) Measurement of antibody graft rate with an anti-mouse IgG- ELISA kit. (E) Immunohistochemical observation of the SIS and AC-SIS. Scale bar = 50 μm. (F) Gross observation of the SIS and AC-SIS. (G) Characterization of the mechanical properties of the SIS and AC-SIS. *$P < 0.05$. (H) Representative SEM image of the surface of the SIS and AC-SIS. Scale bar = 20 μm. (I) Measurement of water contact angle of the SIS and AC-SIS. (J) Quantification of water contact angle of the SIS and AC-SIS.

was crosslinked with various concentrations of CD29 antibody (5–20 μg/mL), and the optimal antibody concentration (10 μg/mL) was determined with the residual sulfhydryl concentration (Fig. 3B). As shown by the subsequent experiments, the results showed no significant cytotoxic effect on the proliferation of the USCs (Fig. 3C). The grafting ratio, as measured with an anti-mouse IgG-ELISA kit, was 72% (Fig. 3D). The immunohistochemical assay also proved that the SIS had been successfully cross-linked with the antibody (Fig. 3E).

As shown in Fig. 3F, there was no obvious morphological change before and after the crosslinking, though the cross-linking has resulted in a slight change in the microstructure of the materials. Analyzing the surface with SEM showed that both SIS and AC-SIS had a porous structure with randomly coiled collagen fibers at the submucosal surface, while the interstitial space of the AC-SIS was slightly reduced without directional change (Fig. 3H). The average contact angle has increased from 61.46 ± 4.87° (SIS group) to 74.73 ± 6.39° (AC-SIS group) after the antibody cross-linking, albeit no statistical difference was detected between the two groups (Fig. 3I and J). Further characterization of the mechanical properties of the SIS and AC-SIS indicated that the elastic moduli is slightly increased in the AC-SIS group as the pore size of collagen bundles decreased (Fig. 3G).

3.2. Characterization and identification of the USCs

The USCs were isolated and cultured as previously described [23,33,35]. Primary cell colonies had appeared after about 1 week, and reached 80% confluence in about 2 weeks (Fig. 4A). Cells from passage 3 were used for subsequent experiments (Fig. 4A).

Flow cytometry was used to analyze the expression ratio of the surface antigens. The USCs were highly positive (≥99%) for CD29, CD44 and CD73, moderately positive (~45.3%) for CD90, and negative for CD133 and CD34 expression (Fig. 4B).

The USCs were cultured in the osteogenic and adipogenic induction medium for 30 days and in chondrogenic induction medium for 24 days, and subsequently stained by Alizarin red staining, Oil red O, or toluidine blue staining, respectively (Fig. 4C).

Thereafter, the USCs were induced with urothelial-inducing medium for 21 days or fibroblastic-inducing medium for 28 days, with epithelial origin marker (AE1/AE3) (Fig. 4D) and smooth muscle markers (α-SMA, Myosin) detected (Fig. 4E).

3.3. Ability of the AC-SIS for capturing the USCs in vitro

To verify whether adherence and proliferation of the USCs could be facilitated by the AC-SIS, we have evaluated the ability of the AC-SIS to capture the USCs under static condition. As the AC-SIS could capture more USCs cells, the number of cells in this group was significantly greater than that in the SIS group after 1 day (Fig. 5B). The survival and proliferation of the captured USCs were evaluated by FACS, CCK-8 assay and calcein-AM staining. As indicated by flow cytometry, there was no difference in the survival of the USCs between the SIS and AC-SIS groups (Fig. 5D), suggesting that the AC-SIS did not induce apoptosis. The results of CCK-8 and calcein-AM staining both indicated that, compared with the SIS group, the USCs had proliferated better on the AC-SIS after 3 and 5 days (Fig. 5B and C). The morphology of the USCs on the surface of different materials was also observed by SEM. As previously reported, the growth of the USCs may be affected by the make and surface morphology of the scaffolds [36,37]. As a loose and porous acellular matrix material, the SIS did not alter the construct of the scaffolds after the cross-linking. Under the SEM, the USCs have displayed a long spindle-like morphology and sound adhesion and growth on the surface of both groups, with the cells aggregated more closely in the AC-SIS group (Fig. 5A).

The function of the bladder is to collect, temporary store and void urine. Normal urine does not contain any cells except a small number of USCs. Therefore, the ability to capture the USCs in the urine may be used as an important indicator for the capturing ability of the scaffold. Supplementary material video has shown the equipment for testing the capability of the scaffolds for capturing the USCs under a dynamic condition. Through flow culturing, all groups have a few USCs adhered at a rotational speed 10 rpm, but confocal images have shown that, compared with the SIS, significantly more USCs have adhered to the surface of the AC-SIS (Fig. 5E). As reported previously, cytoskeletal structures are closely related to cell morphology and spreading, and cytoskeleton disorganization may affect cell proliferation [38,39]. As shown by the cytoskeleton staining in this study, the USCs were stretched and intact, and have adhered and proliferated normally on the surface of both SIS and AC-SIS (Fig. 5F). In addition, there were significantly more cells in the AC-SIS group compared with the SIS group after 6 h.

3.4. Macroscopic observation and histological analysis of the rabbit bladder repair

The AC-SIS was subsequently implanted into a full-thickness bladder defect to evaluate its potential as a bladder patch. The animals were divided into the control group (direct suturing the defect area), SIS group, and AC-SIS group. Bladder tissue of the repair area was collected at various time points (1, 2, 4 and 8 weeks after the operation).

The gross pathology of the bladder tissues was observed after the sampling (Fig. 6A). Adhesion of the sutured area of the bladder to the abdominal wall was noted after 1, 2 and 4 weeks (data not shown). One week after the surgery, the wounds of the control group were almost completely healed, whilst other groups have shown complete coverage by the materials. The SIS and AC-SIS groups showed notable shrinkage and no significant degradation, yet the contracture rate has decreased, and the degradation rate has increased with the elapse of time (Fig. 6A). Two weeks after the operation, the lateral (serosal layer) of the repair region was basically healed in both the SIS and AC-SIS groups, with the tissues showing significantly thickening and submucosal edema (Fig. 6A). At this time, bladder stones were found around the sutures and on the patches in all experimental groups, but had decreased or even disappeared along with the degradation of sutures and/or the material. All implanted materials showed visible degradation 4 weeks after the operation, with the average thickness of the repaired area being greater in all experiment groups, and that of the AC-SIS group being the thickest (Fig. 6A). All experimental groups had healed after 8 weeks. As shown in Fig. 6B, the bladder wall of the control group became thinner during bladder filling, and the bladder size (mean short and long axis = 5.5 cm × 7 cm) was significantly increased with slightly poorer elasticity compared with the normal tissue (mean short and long axis = 4.5 cm × 5.75 cm), while the SIS group had the greatest bladder size (mean short and long axis = 7.5 cm × 6.2 cm). Among the three groups, the bladder wall of the AC-SIS group still had a certain thickness, and the bladder size was closest to the normal (mean short and long axis = 5 cm × 5.3 cm).

The effect of bladder repair by the AC-SIS was further evaluated by histology analysis. As shown by H&E staining, a large number of neovasculature was noted in the area near the edge of the defect 1 week after the operation. In the control group, epithelial and vascular progression had appeared in the submucosa after 2 weeks (Fig. 6C). Meanwhile, a small amount of epithelium had appeared at the edge of repair area in the SIS group, while a large number of neovascular and new epithelial cell masses had appeared in the AC-SIS group (Fig. 6C). 8 weeks after the operation, the regenerated epithelium at the defect area had become multilayered in all groups. However, the control group and the SIS group both lacked the normal fluctuation of bladder urothelium with disordered smooth muscle-like tissues. As expected, the AC-SIS groups showed a normal tissue organization with distinct hierarchical structure and obvious smooth muscle fibers, urothelium layer had loop fluctuations (Fig. 6C), which resembled the normal bladder urothelium (Fig. S2A).

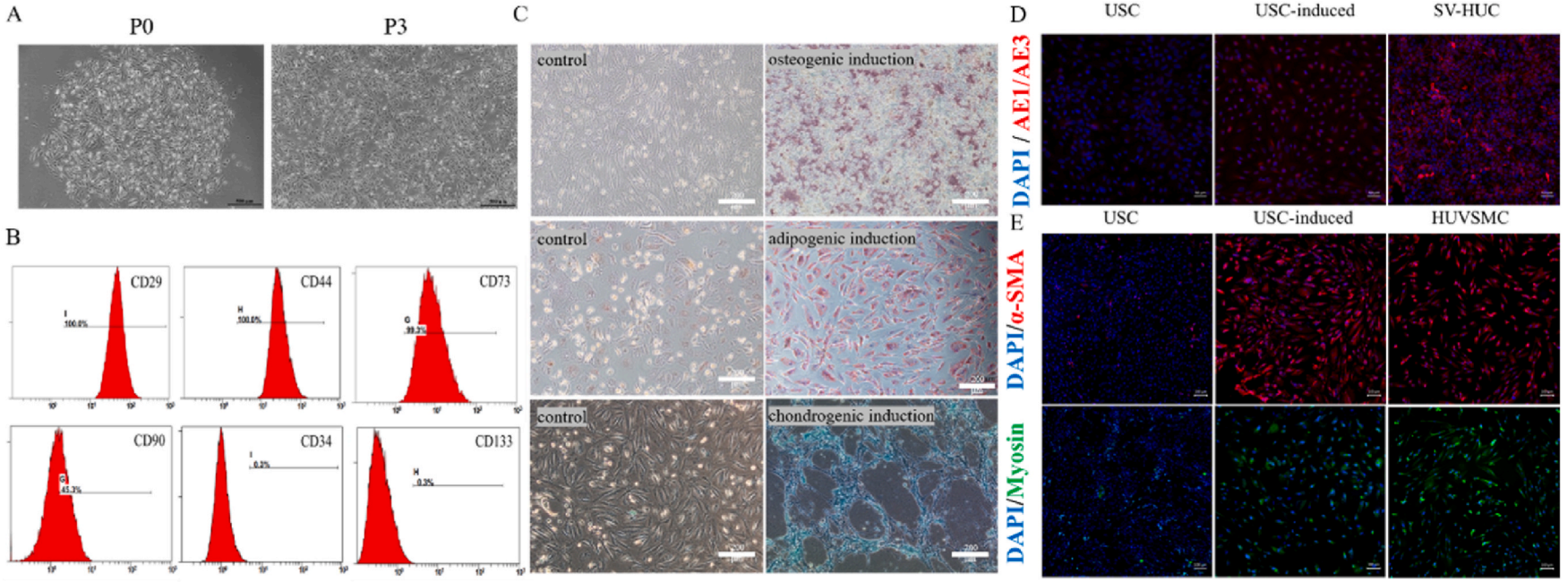

Fig. 4. Characterization of human USCs. (A) Morphology and proliferation of the USCs. Scale bar = 500 μm. (B) Expression of surface marker of the USCs. (C) Representative images of non-induced cells (control group) and osteogenic-induced, adipogenic-induced and chondrogenic-induced USCs. Scale bar = 200 μm. (G) Urothelial differentiation of the USCs with AE1/AE3. SV-HUC was used as positive control, with non-induced USCs showing no fluorescence signal. Scale bar = 50 μm. (H) Myogenic differentiation of the USCs with expression of α-SMA and Myosin. HUVSMC was used as positive control, with non-induced USCs showing no fluorescence signal. Scale bar = 100 μm.

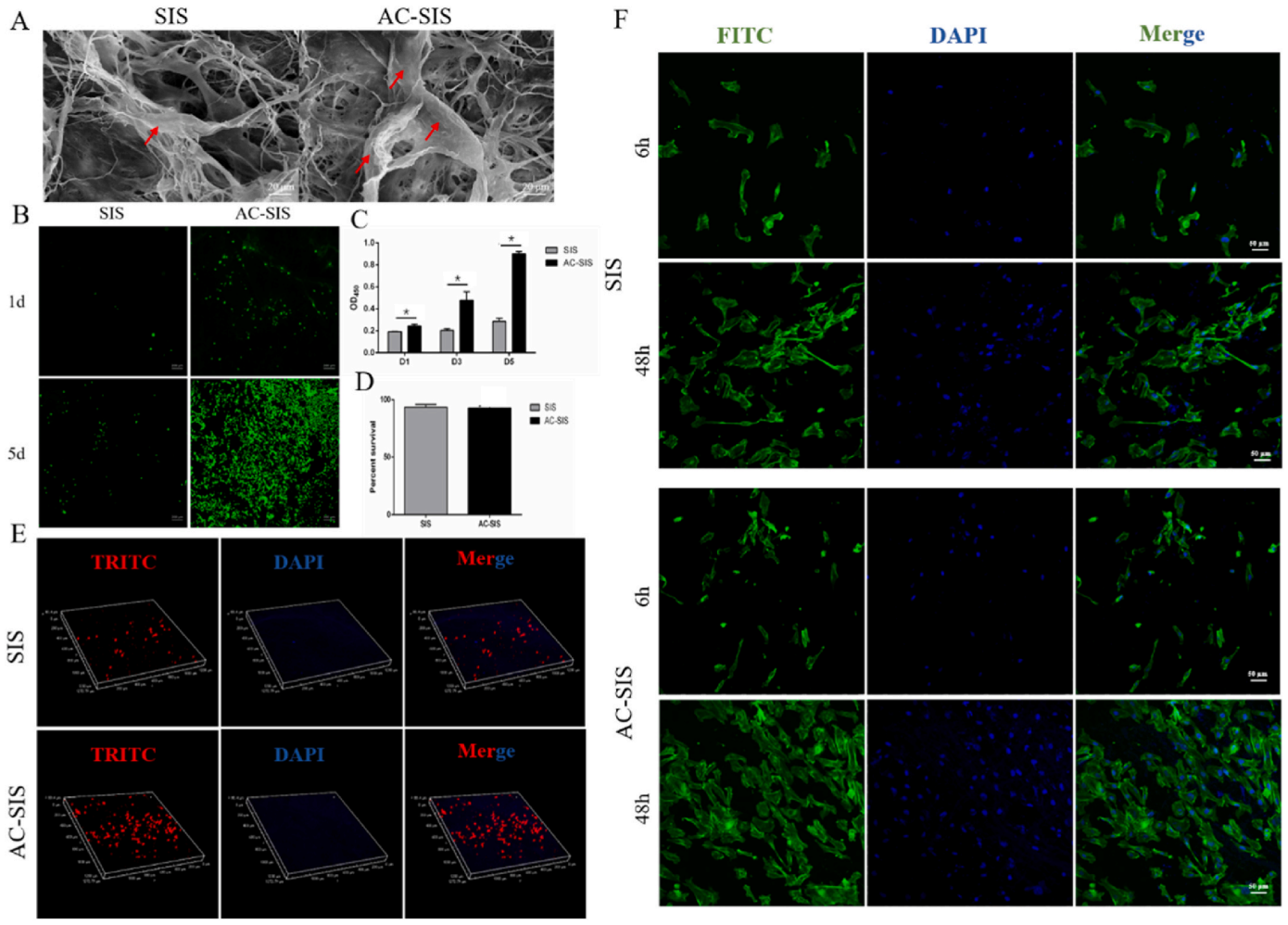

Fig. 5. The capability of the SIS and AC-SIS to capture the USCs *in vitro* (A) Ultrastructure of the USCs on the surface of the SIS and AC-SIS after 3 days of culture. Scale bar = 20 μm. (B) Photographs of the USCs captured by the SIS and AC-SIS under static condition as stained with calc-xanthocyanin. Live cells were stained with calcein AM (green). Scale bar = 200 μm. (C) Proliferation of the USCs captured by the AC-SIS as detected with a Cell Titer 96 kit. $^*P < 0.05$. (D) Flow cytometric analysis of cell apoptosis. (E) Confocal microscopy images of CM-Dil-labeled USCs (red) captured under dynamic condition on the SIS and AC-SIS after 24 h. Scale bar = 200 μm. (F) Phalloidin staining of the cytoskeleton of the USCs captured under a dynamic condition on the SIS and AC-SIS after 6 and 48 h. FITC-phalloidin staining (green) marked the cytoskeleton and DAPI staining (blue) marked the nuclei. Scale bar = 50 μm.

Masson staining also confirmed similar results. 4 weeks after the operation, a large number of collagen formation was observed in the AC-SIS and SIS groups, both with a collagen density significantly higher than that of the control group (Fig. 6C). This may be attributed to that the AC-SIS has captured the USCs and altered the microenvironment, which accelerated the degradation of the AC-SIS. 4 weeks after the operation, small longitudinal and/or circular muscle bands were observed in the AC-SIS group, which was significantly higher in organization hierarchy and regenerated structure as compared with other groups (Fig. 6C). The difference was more pronounced with the elapse of time. 8 weeks after the operation, the control group has closely packed and regularly arranged collagen without muscle fibers, while the SIS group has some loosely distributed smooth muscle bundles (Fig. 6C). In the AC-SIS group, the proportion of collagen fiber area has increased, in addition with prominent smooth muscle bundles.

3.5. Immunofluorescence observation for the repair of rabbit bladder

IF staining has shown regeneration of bladder epithelium (AE1/AE3) and smooth muscle (α-SMA and Myosin) at various time points. Inconsistent with the H&E and Masson staining results, AE1/AE3 staining showed that neo-epithelial cell masses have appeared in submucosa and traveled along to mucosa layers in all three groups 2 weeks after the surgery (Fig. 7A). Four weeks after the surgery, many epithelial cell masses may still be found in the submucosa of the control group but were completely covered by epithelium (Fig. 7A). However, with the epithelial repair nearly completed, the number of neo-epithelial cell masses have decreased and epithelial thickness have peaked in the experiment groups, with the AC-SIS group being the thickest. With the elapse of time, both the SIS and AC-SIS groups have shown a significant decrease of epithelial thickness, which became close to normal after 8 weeks (Fig. 7A). At this point, complete and continuous epithelial structure have formed in all three groups, with the morphology of the AC-SIS group more similar to the normal (Fig. S2C), suggesting a better re-epithelization (Fig. 7A and B).

As shown by muscle staining, the α-SMA and Myosin signals began to overlap after 4 weeks in both groups (Fig. 7B). Compared with the SIS group, the intensity and area of the α-SMA signals were significantly higher in the AC-SIS group after 4 weeks. At week 8, the α-SMA and Myosin signals of the control group and the SIS group were still weak and without a regular structure, while the AC-SIS group has exhibited tightly arranged smooth muscle clusters with a certain size, which indicated gradual maturation of smooth muscle (Fig. 7B) similar to the normal tissue (Figs. S2D and E).

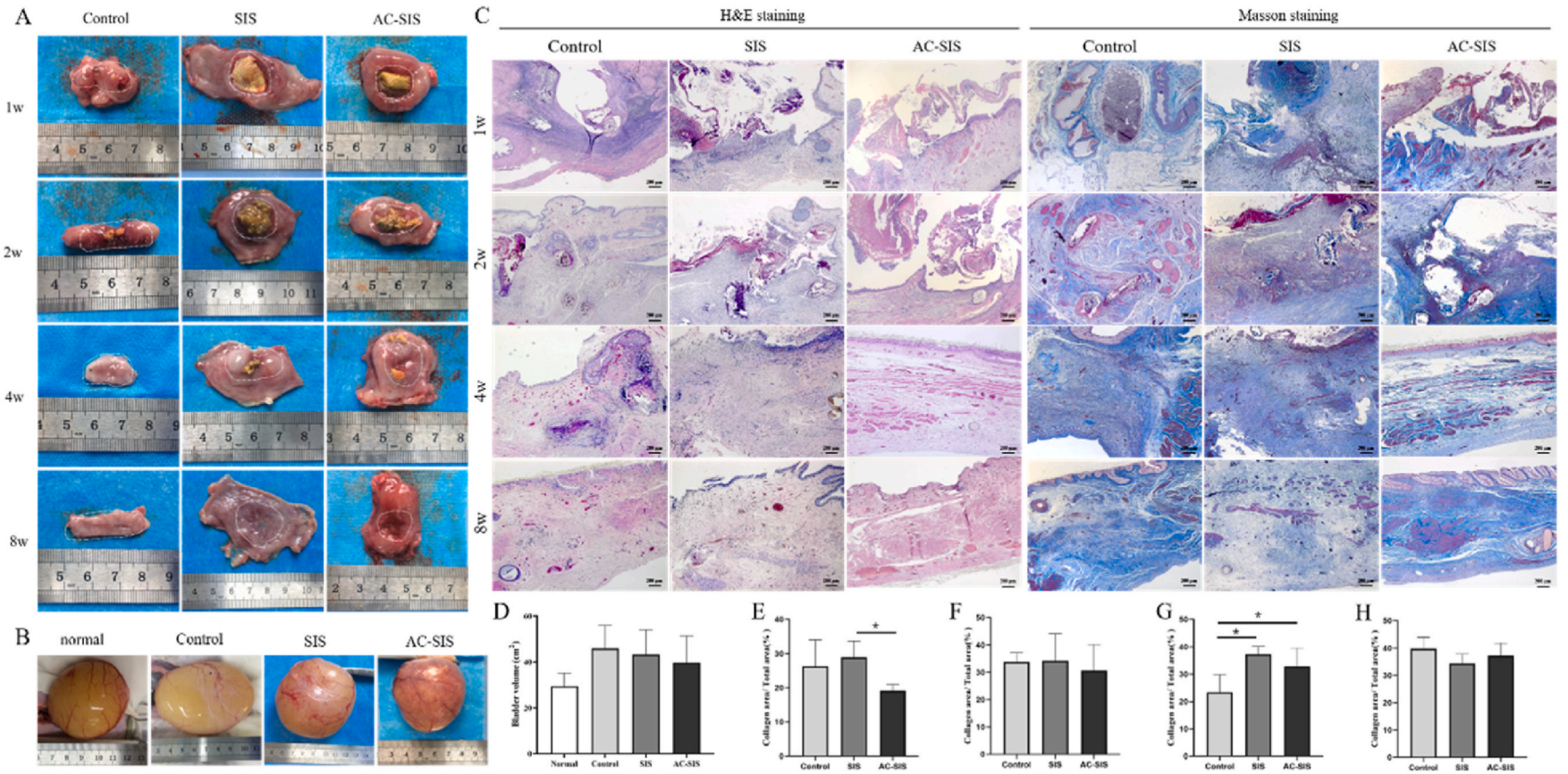

Fig. 6. Macroscopic observation and histological examination of the regenerated bladder. (A) Representative images of the regenerated bladder after 1, 2, 4, and 8 weeks. (B) Representative images of bladder filling at week 8 in various groups. (C) Representative images of H&E staining and Masson staining of the regenerated bladder. Scale bar = 200 μm. (D) Statistical comparison of bladder size in various groups at week 8. Data were presented as mean ± S.D. (E) Comparison of Masson staining for collagen area (%) in each group at week 1. *$P < 0.05$. (F) Comparison of Masson staining for collagen area (%) in each group at week 2. (G) Comparison of Masson staining for collagen area (%) in each group at week 4. *$P < 0.05$. (H) Comparison of Masson staining for collagen area (%) in each group at week 8.

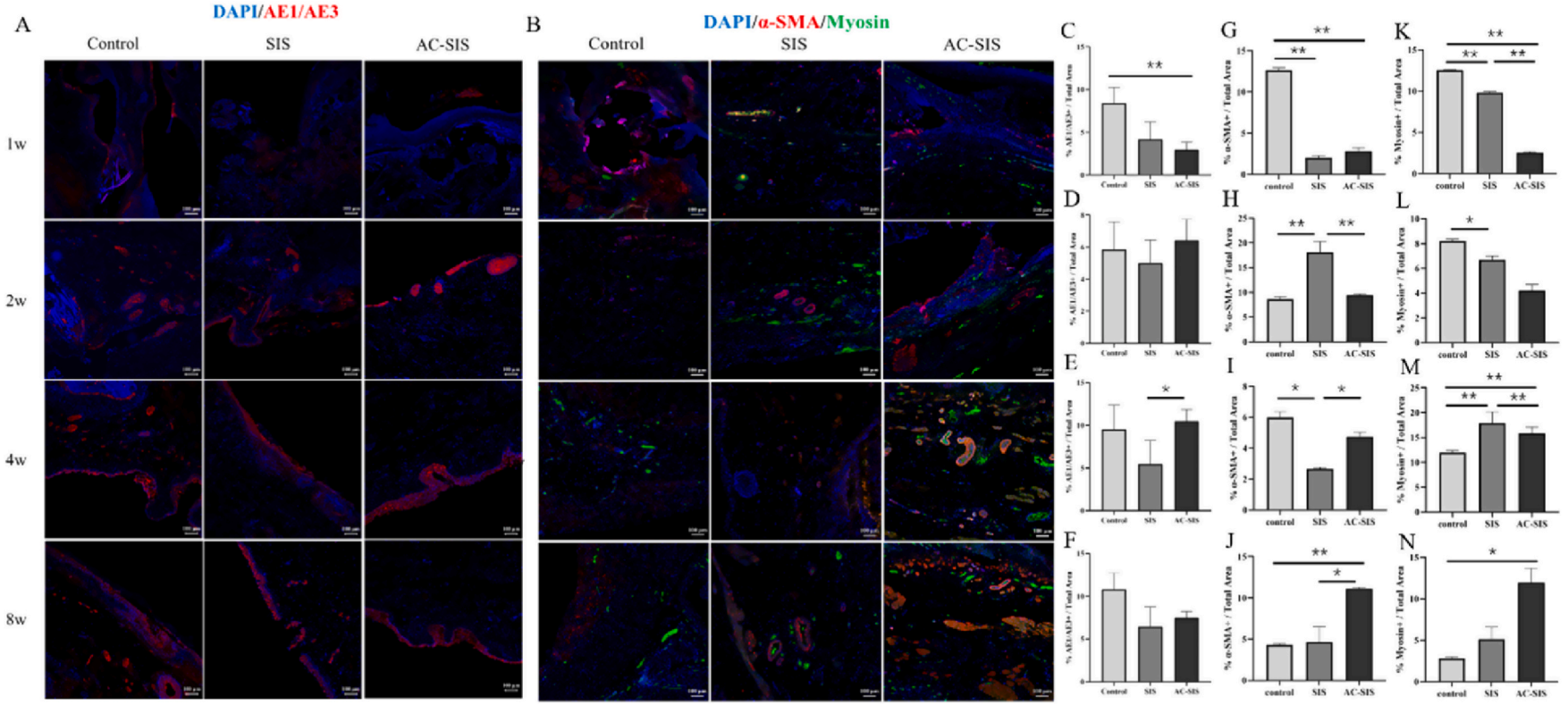

Fig. 7. Immunofluorescence observation of the repaired bladder. (A) Expression of endothelium-associated markers AE1/AE3 in the control and experimental groups. The urothelium was stained with AE1/AE3 (red), while the nuclei were stained with DAPI (blue). Scale bar = 100 μm. (B) Expression of smooth muscle-specific markers α-SMA and Myosin in the control and experimental groups. Bladder and vascular smooth muscle were stained with α-SMA (red) and Myosin (green), the nuclei were stained with DAPI (blue). Scale bar = 100 μm. (C) Percentage of α-SMA positive area relative to the total area of each group as compared after 1 week. Data was presented as mean ± S.D. $^{**}P < 0.01$. (D) Percentage of α-SMA positive area relative to the total area of each group as compared after 2 weeks. Data was presented as mean ± S.D. (E) Percentage of α-SMA positive area relative to the total area of each group as compared after 4 weeks. Data was presented as mean ± S.D. $^{*}P < 0.05$. (F) Percentage of α-SMA positive area relative to the total area of each group as compared after 8 weeks. Data was presented as mean ± S.D. (G) Percentage of α-SMA positive area relative to the total area of each group as compared after 1 week. Data was presented as mean ± S.D. $^{**}P < 0.01$. (H) Percentage of α-SMA positive area relative to the total area of each group as compared after 2 weeks. Data was presented as mean ± S.D. $^{**}P < 0.01$. (I) Percentage of α-SMA positive area relative to the total area of each group as compared after 4 weeks. Data was presented as mean ± S.D. $^{*}P < 0.05$. (J) Percentage of α-SMA positive area relative to the total area of each group as compared after 8 weeks. Data was presented as mean ± S.D. $^{*}P < 0.05$; $^{**}P < 0.01$. (K) Percentage of Myosin positive area relative to the total area of each group as compared after 1 week. Data was presented as mean ± S.D. $^{**}P < 0.01$. (L) Percentage of Myosin positive area relative to the total area of each group as compared after 2 weeks. Data was presented as mean ± S.D. $^{*}P < 0.05$. (M) Percentage of Myosin positive area relative to the total area of each group as compared after 4 weeks. Data was presented as mean ± S.D. $^{**}P < 0.01$. (N) Percentage of Myosin positive area relative to the total area of each group as compared after 8 weeks. Data was presented as mean ± S.D. $^{*}P < 0.05$.

4. Discussion

Tissue engineering based on stem cells and biomaterials has provided a strategy for the reconstruction of impaired bladder. In this study, an antibody-conjugated SIS (AC-SIS) has been successfully fabricated for capturing the USCs for bladder defect repair.

Acellular matrices have provided a unique opportunity for bladder reconstruction in both experimental and clinical set-ups. As a xenogeneic, acellular, biocompatible, biodegradable, and collagen-based scaffold, porcine SIS can enable bladder regeneration without *ex vivo* cell seeding before the implantation [40–43]. The particular biochemical components and excellent mechanical properties have conferred it with appropriate structure and microenvironment not only as a scaffold but also with specific physiological functions suitable for cell adhesion, proliferation, differentiation, and the ultimate tissue regeneration [35,44–53].

Scaffolds as a carrier for stem cells are effective tools for tissue regeneration and repair. As progenitor cells derived from the urinary system, the USCs can be isolated readily from urine and expand extensively through culturing [54]. Such cells possess the desired regenerative properties including robust proliferative capacity [55], multipotential for differentiation [56–60], paracrine effect [61–63], and immune-modulatory property [29], and have been tested in animal models for a multitude of human diseases [29,64–68]. Previous studies have also demonstrated that the USCs could differentiate into multiple bladder cell lineages identifiable by particular gene and/or protein markers, and provide an ideal cell source for the reconstruction of urinary tract [12,57,69,70]. With the potential for urothelial and smooth muscle differentiation, the USCs have offered an unlimited source of cells for tissue remodeling, engineering and regeneration. As illustrated by our *in vitro* study, such cells can efficiently differentiate into urothelial cells and smooth muscle cells within the induction medium.

To seed the USCs onto the SIS for the repair of tissue defects has achieved satisfactory outcome and better efficacy compared with transplantation of the USCs or SIS alone [10,12,70,71]. However, due to the pH value and flowing environment, to directly seed the USCs onto the SIS membrane may result in rapid cell death and reduced therapeutic effect. Furthermore, potential tumorigenicity and immunologic rejection caused by exogenous stem cells transplantation have also raised much concern over its clinical safety. Autologous stem cells for regenerative medicine are ethically more acceptable and likely to be exempted from most of the complications. Due to the relative long period of *in vitro* cultivation and decreased stemness and differentiation potential over time, exogenous cells often cannot fulfill the actual demand. In the present study, a CD29 antibody-conjugated SIS (AC-SIS) has been fabricated to specifically capture own USCs for bladder repair, with the efficacy proven by *in vitro* study.

Targeted capture of cells requires presence of specific membrane antibodies. Isolated from urine samples, subpopulations of the USCs are characterized by distinct cell morphology, various potential for proliferation and differentiation [33], similar clone-forming efficiency and high level of CD29 expression [34]. Also known as Integrin beta 1, an adhesion molecule, the CD29 can bind with a variety of ligands and play an important role in the mobilization, homing, migration and differentiation of stem cells as well as mediation of niche interactions [72–77]. As a surface marker for the MSCs, CD29 is essential for cell adhesion and recognition in a variety of biological processes including embryogenesis, tissue repair and immune response [78,79]. Since no single specific marker has been identified for the USC, we have chosen CD29 as a distinctive target for the capture of the USCs in this study.

In this study, we have adopted the Traut's reagent and Sulfo-SMCC to covalently bind the CD29 with the SIS scaffold. This not only has attained a high cross-linking rate (72%), but also maintained the safety and biocompatibility of the SIS scaffold. As discovered by previous studies, scaffolds treated with the Traut's reagent and Sulfo-SMCC could also improve the vascularization and cellularization, whilst decrease the rate of degradation, which are beneficial for tissue regeneration [80–82]. As shown with our *in vitro* experiments, the CD29 antibody could specifically recognize both the hUSCs and rUSCs (Fig. S3). Better still, the cells captured by the AC-SIS membrane have maintained their activity and a better proliferation capacity compared with the SIS alone.

Therapeutic interventions for bladder defects aim to restore the physiological structure and functions by restoring the urothelial and muscular architecture. As indicated by gross observation, structural integrity and endothelial intactness were presented in all groups 8 weeks after the operation. As revealed by H&E and IF staining, complete urothelium regeneration had occurred within 8 weeks, but the AC-SIS group in particular had an urothelium layer more similar to the normal tissues at the defect area compared with the sham and the SIS groups. The urothelium might have developed from cells migrating from the surrounding native tissues or the captured stem cells. The coordination of blood vessel and smooth muscle growth during the bladder wall regeneration also played a key role in the restoration of bladder function. Re-vascularization is crucial for the implanted patch to provide sufficient blood supply. Regeneration of smooth muscle is crucial to maintain the structural and functional integrity of the bladder. With unsatisfactory bladder muscular wall regeneration, shrinkage, perforation and/or leakage may occur. As revealed by H&E and IF staining, the AC-SIS group had better regeneration of blood vessels and exclusive growth of smooth muscles compared with the SIS group. Such muscle bundles may facilitate the storage and/or urination and maintenance of proper intravesical pressure with an increased amount of urine.

It was reported previously that more than 99.9% of rabbit USCs (rUSCs) are positive for CD29 [34]. Hence, we have selected CD29 as an adhesive medium for the capture of the USCs. For *in vitro* experiment, we have designed two capture models (static and dynamic conditions) to verify the capturing ability of the AC-SIS. In both models, the number of USCs on the AC-SIS was significantly more compared with the control group. As mesenchymal stem cells derived from the urinary system, the USCs have demonstrated the ability to differentiate into various urological and cell lineages as well as to suppress oxidative stress, inflammatory and apoptotic processes. Such cells therefore may provide a potential source for bladder repair [83–87]. Theoretically, it may be feasible to capture more USCs with the AC-SIS to repair bladder damages. Similarly, *in vivo* experiments also confirmed that the AC-SIS could attain a better effect for the repair of bladder epithelium and smooth muscle and for angiogenesis. However, the repair process may be considerably more complex due to the complexity of the *in vivo* environment. With the specificity of CD29, the AC-SIS may capture multiple cell types *in vivo*. However, given that the AC-SIS predominantly make contacts with urine, the target cell population may also include urine-derived epithelial cells, red blood cells and white blood cells [88,89], but whether such cells can maintain their proliferation activity in the urine has remained unknown. Our results have shown clear evidence for the capture of the USCs by the AC-SIS *in vitro* and repairing of rabbit bladder defect *in vivo*. However, to what extent the USCs can be effectively captured by the AC-SIS *in vivo* and which pathways may be involved in the bladder repair by the captured-USCs still await further exploration.

Instead of to seed exogenous cells directly onto the scaffolds, an endogenous stem cells capturing composite scaffold has been constructed. The cell capturing capacity of the scaffolds was evaluated *in vitro* and further tested in an animal model. As shown by the results, specific capture could be integrated into the design and practice of bladder reconstruction. Our study has several limitations. First, the specific capturing capacity has not been evaluated *in vivo*. Second, the captured stem cells have not been traced further on the membrane. Last but not least, longer period of observation, further evaluation of functional recovery, and more detailed mechanism exploration should be considered.

5. Conclusion

In this study, we have fabricated an effective and specific stem cell capturing scaffold (AC-SIS), which showed sound biocompatibility and pro-proliferative effect *in vitro*. As demonstrated with the animal model, the AC-SIS has attained better outcomes for the repair of bladder defect in terms of epithelium and smooth muscle regeneration. This has opened a new revenue for the design and application of bladder reconstruction scaffolds based on capture of particular stem cells for tissue regeneration.

CRediT authorship contribution statement

Yu-Ting Song: Formal analysis, Methodology, Data curation, Writing – original draft. **Yan-Qing Li:** Formal analysis, Methodology, Data curation, Writing – original draft. **Mao-Xuan Tian:** Methodology, Formal analysis, Writing – original draft. **Jun-Gen Hu:** Conceptualization, Formal analysis, Writing – original draft. **Xiu-Ru Zhang:** Methodology, Formal analysis. **Peng-Cheng Liu:** Formal analysis, Writing – original draft. **Xiu-Zhen Zhang:** Methodology. **Qing-Yi Zhang:** Methodology. **Li Zhou:** Methodology. **Long-Mei Zhao:** Methodology. **Jesse Li-Ling:** Formal analysis, Writing – original draft. **Hui-Qi Xie:** Conceptualization, Formal analysis, Writing – original draft, Funding acquisition.

Declaration of competing interest

The authors declare that they have no known competing financial interests or personal relationships that could have appeared to influence the work reported in this paper.

Acknowledgments

This work was supported by the National Natural Science Foundation of China (Grant No. 32171351; 31771065), National Key Research and Development Program of China (Grant No. 2017YFC1104702), and the “1.3.5” Project for Disciplines of Excellence, West China Hospital, Sichuan University (Grant No. ZYJC18002).

Appendix A. Supplementary data

Supplementary data to this article can be found online at https://doi.org/10.1016/j.bioactmat.2021.11.017.

References

[1] S. Xiong, J. Wang, W. Zhu, K. Yang, G. Ding, X. Li, D.D. Eun, Onlay repair technique for the management of ureteral strictures: a comprehensive review, BioMed Res. Int. 2020 (2020), 6178286, https://doi.org/10.1155/2020/6178286.
[2] G. Romagnoli, M. De Luca, F. Faranda, R. Bandelloni, A.T. Franzi, F. Cataliotti, R. Cancedda, Treatment of posterior hypospadias by the autologous graft of cultured urethral epithelium, N. Engl. J. Med. 323 (8) (1990) 527–530, https://doi.org/10.1056/NEJM199008233230806.
[3] M. Vaegler, S. Maurer, P. Toomey, B. Amend, K.D. Sievert, Tissue engineering in urothelium regeneration, Adv. Drug Deliv. Rev. 82–83 (2015) 64–68, https://doi.org/10.1016/j.addr.2014.11.021.
[4] S. Lima, L. Araujo, F.O. Vilar, R. Lima, R. Lima, Nonsecretory intestinocystoplasty: a 15-year prospective study of 183 patients, J. Urol. 179 (3) (2008) 1113–1116, https://doi.org/10.1016/j.juro.2007.10.094, discussion 1116-7.
[5] M. Abdel-Azim, A. Abdel-Hakim, Gastrocystoplasty in patients with an areflexic low compliant bladder, Eur. Urol. 44 (2) (2003) 260–265, https://doi.org/10.1016/s0302-2838(03)00260-4.
[6] J. Budzyn, H. Trinh, S. Raffee, H. Atiemo, Bladder augmentation (Enterocystoplasty): the current state of a historic operation, Curr. Urol. Rep. 20 (9) (2019) 50, https://doi.org/10.1007/s11934-019-0919-z.
[7] L. Hoen, H. Ecclestone, B. Blok, G. Karsenty, V. Phé, R. Bossier, J. Groen, D. Castro-Diaz, B. Padilla Fernández, G. Del Popolo, S. Musco, J. Pannek, T. Kessler, T. Gross, M. Schneider, R. Hamid, Long-term effectiveness and complication rates of bladder augmentation in patients with neurogenic bladder dysfunction: a systematic review, Neurourol. Urodyn. 36 (7) (2017) 1685–1702, https://doi.org/10.1002/nau.23205.
[8] J. Adamowicz, M. Pokrywczynska, S. Van Breda, T. Kloskowski, T. Drewa, Concise review: tissue engineering of urinary bladder; We still have a long way to go? Stem Cells Transl. Med. 6 (11) (2017) 2033–2043, https://doi.org/10.1002/sctm.17-0101.
[9] F. Ajalloueian, G. Lemon, J. Hilborn, I. Chronakis, M. Fossum, Bladder biomechanics and the use of scaffolds for regenerative medicine in the urinary bladder, Nat. Rev. Urol. 15 (3) (2018) 155–174, https://doi.org/10.1038/nrurol.2018.5.
[10] X. Wan, M.-K. Xie, H. Xu, Z.-W. Wei, H.-J. Yao, Z. Wang, D.-C. Zheng, Hypoxia-preconditioned adipose-derived stem cells combined with scaffold promote urethral reconstruction by upregulation of angiogenesis and glycolysis, Stem Cell Res. Ther. 11 (1) (2020), https://doi.org/10.1186/s13287-020-02052-4, 535-535.
[11] K.R. Shrestha, S.H. Jeon, A.R. Jung, I.G. Kim, G.E. Kim, Y.H. Park, S.H. Kim, J. Y. Lee, Stem cells seeded on multilayered scaffolds implanted into an injured bladder rat model improves bladder function, Tissue Eng. Regen. Med. 16 (2) (2019) 201–212, https://doi.org/10.1007/s13770-019-00187-x.
[12] Y. Liu, W. Ma, B. Liu, Y. Wang, J. Chu, G. Xiong, L. Shen, C. Long, T. Lin, D. He, D. Butnaru, L. Alexey, Y. Zhang, D. Zhang, G. Wei, Urethral reconstruction with autologous urine-derived stem cells seeded in three-dimensional porous small intestinal submucosa in a rabbit model, Stem Cell Res. Ther. 8 (1) (2017) 63, https://doi.org/10.1186/s13287-017-0500-y.
[13] G. Jack, R. Zhang, M. Lee, Y. Xu, B. Wu, L. Rodríguez, Urinary bladder smooth muscle engineered from adipose stem cells and a three dimensional synthetic composite, Biomaterials 30 (19) (2009) 3259–3270, https://doi.org/10.1016/j.biomaterials.2009.02.035.
[14] M. Pokrywczynska, M. Rasmus, A. Jundzill, D. Balcerczyk, J. Adamowicz, K. Warda, L. Buchholz, T. Drewa, Mesenchymal stromal cells modulate the molecular pattern of healing process in tissue-engineered urinary bladder: the microarray data, Stem Cell Res. Ther. 10 (1) (2019), https://doi.org/10.1186/s13287-019-1266-1, 176-176.
[15] Q. Wang, D.-D. Xiao, H. Yan, Y. Zhao, S. Fu, J. Zhou, Z. Wang, Z. Zhou, M. Zhang, M.-J. Lu, The morphological regeneration and functional restoration of bladder defects by a novel scaffold and adipose-derived stem cells in a rat augmentation model, Stem Cell Res. Ther. 8 (1) (2017), https://doi.org/10.1186/s13287-017-0597-z, 149-149.
[16] M. Pokrywczynska, A. Jundzill, K. Warda, L. Buchholz, M. Rasmus, J. Adamowicz, M. Bodnar, A. Marszalek, A. Helmin-Basa, J. Michalkiewicz, M. Gagat, A. Grzanka, M. Frontczak-Baniewicz, A.M. Gastecka, T. Kloskowski, M. Nowacki, C. Ricordi, T. Drewa, Does the mesenchymal stem cell source influence smooth muscle regeneration in tissue-engineered urinary bladders? Cell Transplant. 26 (11) (2017) 1780–1791, https://doi.org/10.1177/0963689717722787.
[17] M.H. Amer, F. Rose, K.M. Shakesheff, M. Modo, L.J. White, Translational considerations in injectable cell-based therapeutics for neurological applications: concepts, progress and challenges, NPJ Regen. Med. 2 (2017) 23, https://doi.org/10.1038/s41536-017-0028-x.
[18] M. Rahman, X. Peng, X. Zhao, H. Gong, X. Sun, Q. Wu, D. Wei, 3D bioactive cell-free-scaffolds for in-vitro/*in-vivo* capture and directed osteoinduction of stem cells for bone tissue regeneration, Bioact. Mater. 6 (11) (2021) 4083–4095, https://doi.org/10.1016/j.bioactmat.2021.01.013.
[19] C. Feng, D. Mao, C. Lu, Q. Zhang, X. Liu, Q. Wu, X. Gong, G. Chen, X. Zhu, Single-cell analysis of highly metastatic circulating tumor cells by combining a self-folding induced release reaction with a cell capture microchip, Anal. Chem. 93 (2) (2021) 1110–1119, https://doi.org/10.1021/acs.analchem.0c04156.
[20] Y. Xu, W. Ding, S. Li, C. Li, D. Gao, B. Qiu, A single-cell identification and capture chip for automatically and rapidly determining hydraulic permeability of cells, Anal. Bioanal. Chem. 412 (19) (2020) 4537–4548, https://doi.org/10.1007/s00216-020-02704-7.
[21] Z. Li, D. Shen, S. Hu, T. Su, K. Huang, F. Liu, L. Hou, K. Cheng, Pretargeting and bioorthogonal click chemistry-mediated endogenous stem cell homing for heart repair, ACS Nano 12 (12) (2018) 12193–12200, https://doi.org/10.1021/acsnano.8b05892.
[22] D. Zhang, G. Wei, P. Li, X. Zhou, Y. Zhang, Urine-derived stem cells: a novel and versatile progenitor source for cell-based therapy and regenerative medicine, Genes Dis. 1 (1) (2014) 8–17, https://doi.org/10.1016/j.gendis.2014.07.001.
[23] Y. Zhang, E. McNeill, H. Tian, S. Soker, K.E. Andersson, J.J. Yoo, A. Atala, Urine derived cells are a potential source for urological tissue reconstruction, J. Urol. 180 (5) (2008) 2226–2233, https://doi.org/10.1016/j.juro.2008.07.023.
[24] L. Chen, L. Li, F. Xing, J. Peng, K. Peng, Y. Wang, Z. Xiang, Human urine-derived stem cells: potential for cell-based therapy of cartilage defects, Stem Cell. Int. 2018 (2018), 4686259, https://doi.org/10.1155/2018/4686259.
[25] N. Pavathuparambil Abdul Manaph, M. Al-Hawwas, L. Bobrovskaya, P.T. Coates, X.F. Zhou, Urine-derived cells for human cell therapy, Stem Cell Res. Ther. 9 (1) (2018) 189, https://doi.org/10.1186/s13287-018-0932-z.
[26] S. Bharadwaj, G. Liu, Y. Shi, R. Wu, B. Yang, T. He, Y. Fan, X. Lu, X. Zhou, H. Liu, A. Atala, J. Rohozinski, Y. Zhang, Multipotential differentiation of human urine-derived stem cells: potential for therapeutic applications in urology, Stem Cell. 31 (9) (2013) 1840–1856, https://doi.org/10.1002/stem.1424.
[27] J.J. Guan, X. Niu, F.X. Gong, B. Hu, S.C. Guo, Y.L. Lou, C.Q. Zhang, Z.F. Deng, Y. Wang, Biological characteristics of human-urine-derived stem cells: potential for cell-based therapy in neurology, Tissue Eng. 20 (13–14) (2014) 1794–1806, https://doi.org/10.1089/ten.TEA.2013.0584.
[28] S.Y. Chun, H.T. Kim, J.S. Lee, M.J. Kim, B.S. Kim, B.W. Kim, T.G. Kwon, Characterization of urine-derived cells from upper urinary tract in patients with bladder cancer, Urology 79 (5) (2012), https://doi.org/10.1016/j.urology.2011.12.034, 1186 e1-7.

[29] C. Zhou, X.R. Wu, H.S. Liu, X.H. Liu, G.H. Liu, X.B. Zheng, T. Hu, Z.X. Liang, X. W. He, X.J. Wu, L.C. Smith, Y. Zhang, P. Lan, Immunomodulatory effect of urine-derived stem cells on inflammatory bowel diseases via downregulating Th1/Th17 immune responses in a PGE2-dependent manner, J. Crohns Colitis 14 (5) (2020) 654–668, https://doi.org/10.1093/ecco-jcc/jjz200.

[30] S. Bharadwaj, G. Liu, Y. Shi, C. Markert, K.-E. Andersson, A. Atala, Y. Zhang, Characterization of urine-derived stem cells obtained from upper urinary tract for use in cell-based urological tissue engineering, Tissue Eng. 17 (15–16) (2011) 2123–2132, https://doi.org/10.1089/ten.TEA.2010.0637.

[31] D. Qin, T. Long, J. Deng, Y. Zhang, Urine-derived stem cells for potential use in bladder repair, Stem Cell Res. Ther. 5 (3) (2014) 69, https://doi.org/10.1186/scrt458.

[32] T. Zhou, C. Benda, S. Duzinger, Y. Huang, X. Li, Y. Li, X. Guo, G. Cao, S. Chen, L. Hao, Y.C. Chan, K.M. Ng, J.C. Ho, M. Wieser, J. Wu, H. Redl, H.F. Tse, J. Grillari, R. Grillari-Voglauer, D. Pei, M.A. Esteban, Generation of induced pluripotent stem cells from urine, J. Am. Soc. Nephrol. 22 (7) (2011) 1221–1228, https://doi.org/10.1038/nprot.2012.115.

[33] A.J. Chen, J.K. Pi, J.G. Hu, Y.Z. Huang, H.W. Gao, S.F. Li, J. Li-Ling, H.Q. Xie, Identification and characterization of two morphologically distinct stem cell subpopulations from human urine samples, Sci. China Life Sci. 63 (5) (2020) 712–723, https://doi.org/10.1007/s11427-018-9543-1.

[34] H. Yang, B. Chen, J. Deng, G. Zhuang, S. Wu, G. Liu, C. Deng, G. Yang, X. Qiu, P. Wei, X. Wang, Y. Zhang, Characterization of rabbit urine-derived stem cells for potential application in lower urinary tract tissue regeneration, Cell Tissue Res. 374 (2) (2018) 303–315, https://doi.org/10.1007/s00441-018-2885-z.

[35] X.R. Zhang, Y.Z. Huang, H.W. Gao, Y.L. Jiang, J.G. Hu, J.K. Pi, A.J. Chen, Y. Zhang, L. Zhou, H.Q. Xie, Hypoxic preconditioning of human urine-derived stem cell-laden small intestinal submucosa enhances wound healing potential, Stem Cell Res. Ther. 11 (1) (2020) 150, https://doi.org/10.1186/s13287-020-01662-2.

[36] V. Gribova, C.Y. Liu, A. Nishiguchi, M. Matsusaki, T. Boudou, C. Picart, M. Akashi, Construction and myogenic differentiation of 3D myoblast tissues fabricated by fibronectin-gelatin nanofilm coating, Biochem. Biophys. Res. Commun. 474 (3) (2016) 515–521, https://doi.org/10.1016/j.bbrc.2016.04.130.

[37] M.M. Stern, R.L. Myers, N. Hammam, K.A. Stern, D. Eberli, S.B. Kritchevsky, S. Soker, M. Van Dyke, The influence of extracellular matrix derived from skeletal muscle tissue on the proliferation and differentiation of myogenic progenitor cells *ex vivo*, Biomaterials 30 (12) (2009) 2393–2399, https://doi.org/10.1016/j.biomaterials.2008.12.069.

[38] Y. Xin, X. Chen, X. Tang, K. Li, M. Yang, W.C. Tai, Y. Liu, Y. Tan, Mechanics and actomyosin-dependent survival/chemoresistance of suspended tumor cells in shear flow, Biophys. J. 116 (10) (2019) 1803–1814, https://doi.org/10.1016/j.bpj.2019.04.011.

[39] L. Bianchi, A. Gagliardi, S. Maruelli, R. Besio, C. Landi, R. Gioia, K.M. Kozloff, B. M. Khoury, P.J. Coucke, S. Symoens, J.C. Marini, A. Rossi, L. Bini, A. Forlino, Altered cytoskeletal organization characterized lethal but not surviving Brtl+/- mice: insight on phenotypic variability in osteogenesis imperfecta, Hum. Mol. Genet. 24 (21) (2015) 6118–6133, https://doi.org/10.1093/hmg/ddv328.

[40] E. Cheng, B. Kropp, Urologic tissue engineering with small-intestinal submucosa: potential clinical applications, World J. Urol. 18 (1) (2000) 26–30, https://doi.org/10.1007/PL00007071.

[41] F. Zhang, L. Liao, Long-term follow-up of neurogenic bladder patients after bladder augmentation with small intestinal submucosa, World J. Urol. 38 (9) (2020) 2279–2288, https://doi.org/10.1007/s00345-019-03008-x.

[42] F. Zhang, L. Liao, Tissue engineered cystoplasty augmentation for treatment of neurogenic bladder using small intestinal submucosa: an exploratory study, J. Urol. 192 (2) (2014) 544–550, https://doi.org/10.1016/j.juro.2014.01.116.

[43] G. Cao, Y. Huang, K. Li, Y. Fan, H. Xie, X. Li, Small intestinal submucosa: superiority, limitations and solutions, and its potential to address bottlenecks in tissue repair, J. Mater. Chem. B 7 (33) (2019) 5038–5055, https://doi.org/10.1039/c9tb00530g.

[44] L.M. Zhao, M. Gong, R. Wang, Q.J. Yuan, Y. Zhang, J.K. Pi, X.H. Lv, Y. Xie, H. Q. Xie, Accelerating ESD-induced gastric ulcer healing using a pH-responsive polyurethane/small intestinal submucosa hydrogel delivered by endoscopic catheter, Regen. Biomater. 8 (1) (2021), https://doi.org/10.1093/rb/rbaa056 rbaa056.

[45] X.Z. Zhang, Y.L. Jiang, J.G. Hu, L.M. Zhao, Q.Z. Chen, Y. Liang, Y. Zhang, X.X. Lei, R. Wang, Y. Lei, Q.Y. Zhang, J. Li-Ling, H.Q. Xie, Procyanidins-crosslinked small intestine submucosa: a bladder patch promotes smooth muscle regeneration and bladder function restoration in a rabbit model, Bioact. Mater. 6 (6) (2021) 1827–1838, https://doi.org/10.1016/j.bioactmat.2020.11.023.

[46] M. Gou, Y.Z. Huang, J.G. Hu, Y.L. Jiang, X.Z. Zhang, N.C. Su, Y. Lei, H. Zhang, H. Wang, H.Q. Xie, Epigallocatechin-3-gallate cross-linked small intestinal submucosa for guided bone regeneration, ACS Biomater. Sci. Eng. 5 (10) (2019) 5024–5035.

[47] Z.L. Wang, S.Z. Wu, Z.F. Li, J.H. Guo, Y. Zhang, J.K. Pi, J.G. Hu, X.J. Yang, F. G. Huang, H.Q. Xie, Comparison of small intestinal submucosa and polypropylene mesh for abdominal wall defect repair, J. Biomater. Sci. Polym. Ed. 29 (6) (2018) 663–682, https://doi.org/10.1021/acsbiomaterials.9b00920.

[48] M. Wang, Y.Q. Li, J. Cao, M. Gong, Y. Zhang, X. Chen, M.X. Tian, H.Q. Xie, Accelerating effects of genipin-crosslinked small intestinal submucosa for defected gastric mucosa repair, J. Mater. Chem. B 5 (34) (2017) 7059–7071, https://doi.org/10.1039/c7tb00517b.

[49] S.K. He, J.H. Guo, Z.L. Wang, Y. Zhang, Y.H. Tu, S.Z. Wu, F.G. Huang, H.Q. Xie, Efficacy and safety of small intestinal submucosa in dural defect repair in a canine model, Mater. Sci. Eng. C Mater. Biol. Appl. 73 (2017) 267–274, https://doi.org/10.1016/j.msec.2016.12.077.

[50] L. Da, M. Gong, A. Chen, Y. Zhang, Y. Huang, Z. Guo, S. Li, J. Li-Ling, L. Zhang, H. Xie, Composite elastomeric polyurethane scaffolds incorporating small intestinal submucosa for soft tissue engineering, Acta Biomater. 59 (2017) 45–57, https://doi.org/10.1016/j.actbio.2017.05.041.

[51] B. Tan, M. Wang, X. Chen, J. Hou, X. Chen, Y. Wang, J. Li-Ling, H. Xie, Tissue engineered esophagus by copper–small intestinal submucosa graft for esophageal repair in a canine model, Sci. China Life Sci. 57 (2) (2014) 248–255, https://doi.org/10.1007/s11427-013-4603-0.

[52] M.R. Fan, M. Gong, L.C. Da, L. Bai, X.Q. Li, K.F. Chen, J. Li-Ling, Z.M. Yang, H. Q. Xie, Tissue engineered esophagus scaffold constructed with porcine small intestinal submucosa and synthetic polymers, Biomed. Mater. 9 (1) (2014), 015012, https://doi.org/10.1088/1748-6041/9/1/015012.

[53] B. Tan, R. Wei, Z. Yang, X. Li, P. Han, W. Zhi, H. Xie, An experimental study of coculture of esophageal mucosa epithelial cells with SIS and their biological characteristics, Zhongguo Xiu Fu Chong Jian Wai Ke Za Zhi 22 (6) (2008) 742–746.

[54] G. Bento, A. Shafigullina, A. Rizvanov, V. Sardão, M. Macedo, P. Oliveira, Urine-derived stem cells: applications in regenerative and predictive medicine, Cells 9 (3) (2020), https://doi.org/10.3390/cells9030573.

[55] H. Kang, S. Choi, B. Kim, J. Choi, G. Park, T. Kwon, S. Chun, Advanced properties of urine derived stem cells compared to adipose tissue derived stem cells in terms of cell proliferation, immune modulation and multi-differentiation, J. Kor. Med. Sci. 30 (12) (2015) 1764–1776, https://doi.org/10.3346/jkms.2015.30.12.1764.

[56] M. Zhou, L. Shen, Y. Qiao, Z. Sun, Inducing differentiation of human urine-derived stem cells into hepatocyte-like cells by coculturing with human hepatocyte L02 cells, J. Cell. Biochem. 121 (1) (2020) 566–573, https://doi.org/10.1002/jcb.29301.

[57] Z. Zhao, D. Liu, Y. Chen, Q. Kong, D. Li, Q. Zhang, C. Liu, Y. Tian, C. Fan, L. Meng, H. Zhu, H. Yu, Ureter tissue engineering with vessel extracellular matrix and differentiated urine-derived stem cells, Acta Biomater. 88 (2019) 266–279, https://doi.org/10.1016/j.actbio.2019.01.072.

[58] Y. Hwang, S. Cha, Y. Hong, A. Jung, H. Jun, Direct differentiation of insulin-producing cells from human urine-derived stem cells, Int. J. Med. Sci. 16 (12) (2019) 1668–1676, https://doi.org/10.7150/ijms.36011.

[59] G. Liu, R. Wu, B. Yang, C. Deng, X. Lu, S. Walker, P. Ma, S. Mou, A. Atala, Y. Zhang, Human urine-derived stem cell differentiation to endothelial cells with barrier function and nitric oxide production, Stem Cells Transl. Med. 7 (9) (2018) 686–698, https://doi.org/10.1002/sctm.18-0040.

[60] L. Wang, Y. Chen, C. Guan, Z. Zhao, Q. Li, J. Yang, J. Mo, B. Wang, W. Wu, X. Yang, L. Song, J. Li, Using low-risk factors to generate non-integrated human induced pluripotent stem cells from urine-derived cells, Stem Cell Res. Ther. 8 (1) (2017) 245, https://doi.org/10.1186/s13287-017-0698-8.

[61] Q. Zhu, Q. Li, X. Niu, G. Zhang, X. Ling, J. Zhang, Y. Wang, Z. Deng, Extracellular vesicles secreted by human urine-derived stem cells promote ischemia repair in a mouse model of hind-limb ischemia, Cell. Physiol. Biochem. 47 (3) (2018) 1181–1192, https://doi.org/10.1159/000490214.

[62] Y. Zhang, X. Niu, X. Dong, Y. Wang, H. Li, Bioglass enhanced wound healing ability of urine-derived stem cells through promoting paracrine effects between stem cells and recipient cells, J. Tissue Eng. Regen. Med. 12 (3) (2018) e1609–e1622, https://doi.org/10.1002/term.2587.

[63] C. Chen, S. Rao, L. Ren, X. Hu, Y. Tan, Y. Hu, J. Luo, Y. Liu, H. Yin, J. Huang, J. Cao, Z. Wang, Z. Liu, H. Liu, S. Tang, R. Xu, H. Xie, Exosomal DMBT1 from human urine-derived stem cells facilitates diabetic wound repair by promoting angiogenesis, Theranostics 8 (6) (2018) 1607–1623, https://doi.org/10.7150/thno.22958.

[64] X. Ling, G. Zhang, Y. Xia, Q. Zhu, J. Zhang, Q. Li, X. Niu, G. Hu, Y. Yang, Y. Wang, Z. Deng, Exosomes from human urine-derived stem cells enhanced neurogenesis via miR-26a/HDAC6 axis after ischaemic stroke, J. Cell Mol. Med. 24 (1) (2020) 640–654, https://doi.org/10.1111/jcmm.14774.

[65] Y. Chen, Y. Xu, M. Li, Q. Shi, C. Chen, Application of autogenous urine-derived stem cell sheet enhances rotator cuff healing in a canine model, Am. J. Sports Med. 48 (14) (2020) 3454–3466, https://doi.org/10.1177/0363546520962774.

[66] C. Deng, Y. Xie, C. Zhang, B. Ouyang, H. Chen, L. Lv, J. Yao, X. Liang, Y. Zhang, X. Sun, C. Deng, G. Liu, Urine-derived stem cells facilitate endogenous spermatogenesis restoration of Busulfan-induced nonobstructive azoospermic mice by paracrine exosomes, Stem Cell. Dev. 28 (19) (2019) 1322–1333, https://doi.org/10.1089/scd.2019.0026.

[67] J. Li, H. Luo, X. Dong, Q. Liu, C. Wu, T. Zhang, X. Hu, Y. Zhang, B. Song, L. Li, Therapeutic effect of urine-derived stem cells for protamine/lipopolysaccharide-induced interstitial cystitis in a rat model, Stem Cell Res. Ther. 8 (1) (2017) 107, https://doi.org/10.1186/s13287-017-0547-9.

[68] Q. Yang, X. Chen, T. Zheng, D. Han, H. Zhang, Y. Shi, J. Bian, X. Sun, K. Xia, X. Liang, G. Liu, Y. Zhang, C. Deng, Transplantation of human urine-derived stem cells transfected with pigment epithelium-derived factor to protect erectile function in a rat model of cavernous nerve injury, Cell Transplant. 25 (11) (2016) 1987–2001, https://doi.org/10.3727/096368916X691448.

[69] H. Yang, B. Chen, J. Deng, G. Zhuang, S. Wu, G. Liu, C. Deng, G. Yang, X. Qiu, P. Wei, X. Wang, Y. Zhang, Characterization of rabbit urine-derived stem cells for potential application in lower urinary tract tissue regeneration, Cell Tissue Res. 374 (2) (2018) 303–315, https://doi.org/10.1007/s00441-018-2885-z.

[70] Q. Wan, G. Xiong, G. Liu, T. Shupe, G. Wei, D. Zhang, D. Liang, X. Lu, A. Atala, Y. Zhang, Urothelium with barrier function differentiated from human urine-derived stem cells for potential use in urinary tract reconstruction, Stem Cell Res. Ther. 9 (1) (2018) 304, https://doi.org/10.1186/s13287-018-1035-6.

[71] S. Wu, Y. Liu, S. Bharadwaj, A. Atala, Y. Zhang, Human urine-derived stem cells seeded in a modified 3D porous small intestinal submucosa scaffold for urethral

tissue engineering, Biomaterials 32 (5) (2011) 1317–1326, https://doi.org/10.1016/j.biomaterials.2010.10.006.
[72] S. Indumathi, R. Harikrishnan, J.S. Rajkumar, M. Dhanasekaran, Immunophenotypic comparison of heterogenous non-sorted versus sorted mononuclear cells from human umbilical cord blood: a novel cell enrichment approach, Cytotechnology 67 (1) (2015) 107–114, https://doi.org/10.1007/s10616-013-9663-2.
[73] R.H. Liu, Y.Q. Li, W.J. Zhou, Y.J. Shi, L. Ni, G.X. Liu, Supplementing mesenchymal stem cells improves the therapeutic effect of hematopoietic stem cell transplantation in the treatment of murine systemic lupus erythematosus, Transplant. Proc. 46 (5) (2014) 1621–1627, https://doi.org/10.1016/j.transproceed.2014.03.003.
[74] Y. Yang, M. Hu, Y. Zhang, H. Li, Z. Miao, CD29 of human umbilical cord mesenchymal stem cells is required for expansion of CD34 (+) cells, Cell Prolif 47 (6) (2014) 596–603, https://doi.org/10.1111/cpr.12130.
[75] T. Bakhshi, R.C. Zabriskie, S. Bodie, S. Kidd, S. Ramin, L.A. Paganessi, S. A. Gregory, H.C. Fung, K.W. Christopherson, 2nd, Mesenchymal stem cells from the Wharton's jelly of umbilical cord segments provide stromal support for the maintenance of cord blood hematopoietic stem cells during long-term *ex vivo* culture, Transfusion 48 (12) (2008) 2638–2644, https://doi.org/10.1111/j.1537-2995.2008.01926.x.
[76] C. Campagnoli, I.A. Roberts, S. Kumar, P.R. Bennett, I. Bellantuono, N.M. Fisk, Identification of mesenchymal stem/progenitor cells in human first-trimester fetal blood, liver, and bone marrow, Blood 98 (8) (2001) 2396–2402, https://doi.org/10.1182/blood.v98.8.2396.
[77] A. Jiménez-Marín, J.J. Garrido, D.F. de Andrés-Cara, L. Morera, M.J. Barbancho, D. Llanes, Molecular cloning and characterization of the pig homologue to human CD29, the integrin beta1 subunit, Transplantation 70 (4) (2000) 649–655, https://doi.org/10.1097/00007890-200008270-00019.
[78] Y. Wang, F. Wang, H. Zhao, X. Zhang, H. Chen, K. Zhang, Human adipose-derived mesenchymal stem cells are resistant to HBV infection during differentiation into hepatocytes *in vitro*, Int. J. Mol. Sci. 15 (4) (2014) 6096–6110, https://doi.org/10.3390/ijms15046096.
[79] P. Hu, Y. Pu, X. Li, Z. Zhu, Y. Zhao, W. Guan, Y. Ma, Isolation, *in vitro* culture and identification of a new type of mesenchymal stem cell derived from fetal bovine lung tissues, Mol. Med. Rep. 12 (3) (2015) 3331–3338, https://doi.org/10.3892/mmr.2015.3854.
[80] Y. Li, Q. He, X. Hu, Y. Liu, X. Cheng, X. Li, F. Deng, Improved performance of collagen scaffolds crosslinked by Traut's reagent and Sulfo-SMCC, J. Biomater. Sci. Polym. Ed. 28 (7) (2017) 629–647, https://doi.org/10.1080/09205063.2017.1291296.
[81] J. Li, X. Chen, K. Ling, Z. Liang, H. Xu, Evaluation of the bioactivity about anti-sca-1/basic fibroblast growth factor-urinary bladder matrix scaffold for pelvic reconstruction, J. Biomater. Appl. 33 (6) (2019) 808–818, https://doi.org/10.1177/0885328218811390.
[82] H. Sun, J. Wang, F. Deng, Y. Liu, X. Zhuang, J. Xu, L. Li, Co-delivery and controlled release of stromal cell-derived factor-1α chemically conjugated on collagen scaffolds enhances bone morphogenetic protein-2-driven osteogenesis in rats, Mol. Med. Rep. 14 (1) (2016) 737–745, https://doi.org/10.3892/mmr.2016.5339.
[83] J.W. Chung, S.Y. Chun, E.H. Lee, Y.S. Ha, J.N. Lee, P.H. Song, E.S. Yoo, T.G. Kwon, S.K. Chung, B.S. Kim, Verification of mesenchymal stem cell injection therapy for interstitial cystitis in a rat model, PLoS One 14 (12) (2019), e0226390, https://doi.org/10.1371/journal.pone.0226390.
[84] D. Wang, J. Li, Y. Zhang, M. Zhang, J. Chen, X. Li, X. Hu, S. Jiang, S. Shi, L. Sun, Umbilical cord mesenchymal stem cell transplantation in active and refractory systemic lupus erythematosus: a multicenter clinical study, Arthritis Res. Ther. 16 (2) (2014) R79, https://doi.org/10.1186/ar4520.
[85] M. Maumus, D. Guérit, K. Toupet, C. Jorgensen, D. Noël, Mesenchymal stem cell-based therapies in regenerative medicine: applications in rheumatology, Stem Cell Res. Ther. 2 (2) (2011) 14, https://doi.org/10.1186/scrt55.
[86] J.N. Lee, S.Y. Chun, H.J. Lee, Y.J. Jang, S.H. Choi, D.H. Kim, S.H. Oh, P.H. Song, J. H. Lee, J.K. Kim, T.G. Kwon, Human urine-derived stem cells seeded surface modified composite scaffold grafts for bladder reconstruction in a rat model, J. Kor. Med. Sci. 30 (12) (2015) 1754–1763, https://doi.org/10.3346/jkms.2015.30.12.1754.
[87] J. Li, H. Luo, X. Dong, Q. Liu, C. Wu, T. Zhang, X. Hu, Y. Zhang, B. Song, L. Li, Therapeutic effect of urine-derived stem cells for protamine/lipopolysaccharide-induced interstitial cystitis in a rat model, Stem Cell Res. Ther. 8 (1) (2017) 107, https://doi.org/10.1186/s13287-017-0547-9.
[88] C.K. Chen, J. Liao, M.S. Li, B.L. Khoo, Urine biopsy technologies: cancer and beyond, Theranostics 10 (17) (2020) 7872–7888, https://doi.org/10.7150/thno.44634.
[89] C. Grupp, H. John, U. Hemprich, A. Singer, U. Munzel, G.A. Müller, Identification of nucleated cells in urine using lectin staining, Am. J. Kidney Dis. 37 (1) (2001) 84–93, https://doi.org/10.1053/ajkd.2001.20592.